Electronic Supplementary Material (ESI) for New Journal of Chemistry.

Supporting information

Tris functionalized Cu-centered cyclohexamolybdate molecular armor as bimetallic catalyst for rapid *p*-nitrophenol hydrogenation

Qihua Fang[a,b], Junhong Fu[b], Fei Wang[a,*], Zhaoxian Qin[b], Weiguang Ma[b], Jiangwei Zhang[b,*] Gao Li[b]

[a]Advanced Catalysis and Green Manufacturing Collaborative Innovation Center, Changzhou University, Changzhou 213164, P.R. China. E-mail: wangfei@cczu.edu.cn (F.W.)

[b]Gold Catalysis Research Center, State Key Laboratory of Catalysis, Dalian Institute of Chemical Physics, Chinese Academy of Sciences, Dalian 116023, P.R. China. E-mail: jwzhang@dicp.ac.cn (J.Z.)

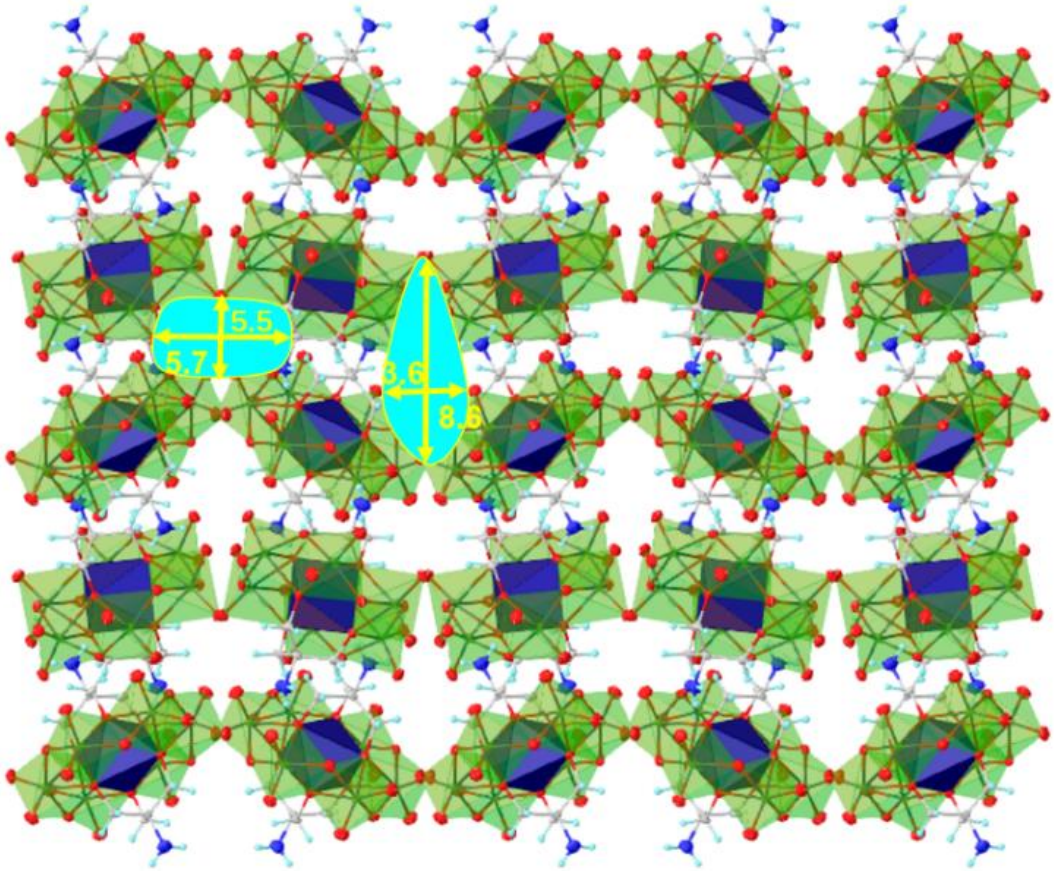

Figure S1. 3D framework structure of [$CuMo_6$] packing along a axis quasi 2D material with atomically dispersed Cu^{2+} in the uniform distance of 11.76 Å and possessing two shapes of nanoporous.

Table S1. Details and results of the BVS calculations Subroutine Calc_BVS (JRC-LLB, version: March-2005). Title: Summary of Bond-Valence calculations for file: $(NH_4)_4\{[NH_2C(CH_2O)_3]_2CuMo_6O_{18}\}$.cfl

Atom	Coord	D_aver Sigm	Distort ($x10^{-4}$)	Valence	BVSum(Sigma)
Mo3	6	1.9113(13)	210.838	6	6.544(31)
Mo2	6	1.9716(13)	132.717	6	5.989(26)
Mo1	6	1.9025(13)	130.535	6	5.942(29)
Cu1	6	2.0384(12)	16.059	2	2.125(8)
O3	4	2.1896(16)	52.276	-2	1.609(8)
O2	4	2.0650(17)	79.692	-2	2.274(12)
O4	2	1.9156(24)	1.738	-2	1.959(12)
O5	2	1.9247(22)	0.254	-2	1.907(11)
O6	2	1.7581(21)	95.508	-2	2.319(20)
O9	1	1.7076(38)	0	-2	1.714(17)
O1	4	2.1995(17)	46.806	-2	1.546(8)
O7	1	1.7022(36)	0	-2	1.740(17)
O10	1	1.7167(34)	0	-2	1.673(15)
O12	1	1.6964(36)	0	-2	1.767(17)
O8	1	1.7301(38)	0	-2	1.613(16)
O11	1	1.7152(34)	0	-2	1.679(15)

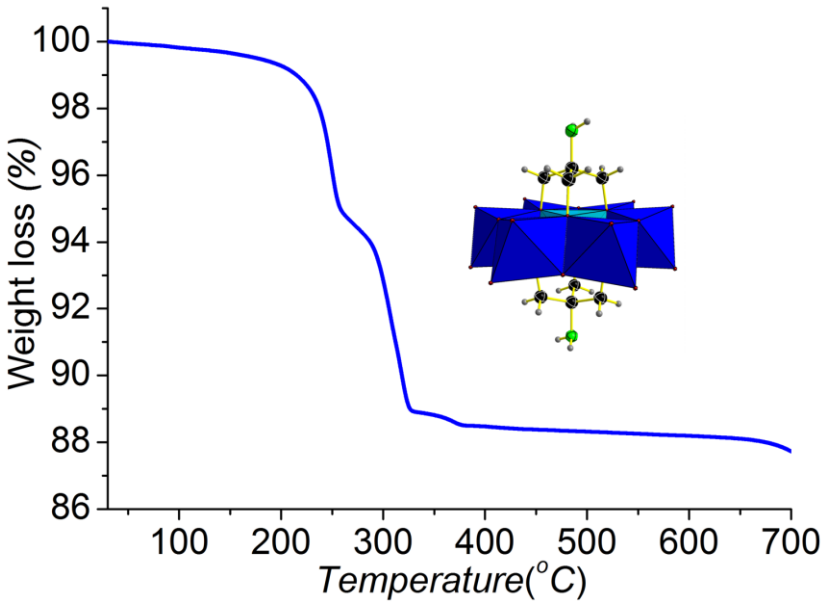

Figure S2. TGA analysis of the $(NH_4)_4\{[NH_2C(CH_2O)_3]_2CuMo_6O_{18}\}$ cluster.

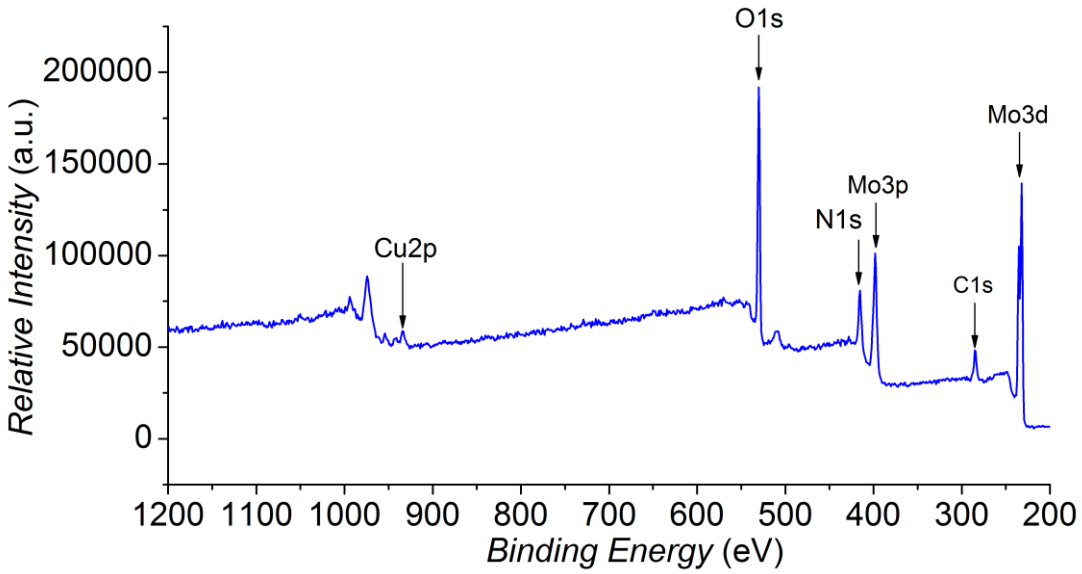

Figure S3. The full XPS spectrum survey of $(NH_4)_4\{[NH_2C(CH_2O)_3]_2CuMo_6O_{18}\}$ cluster.

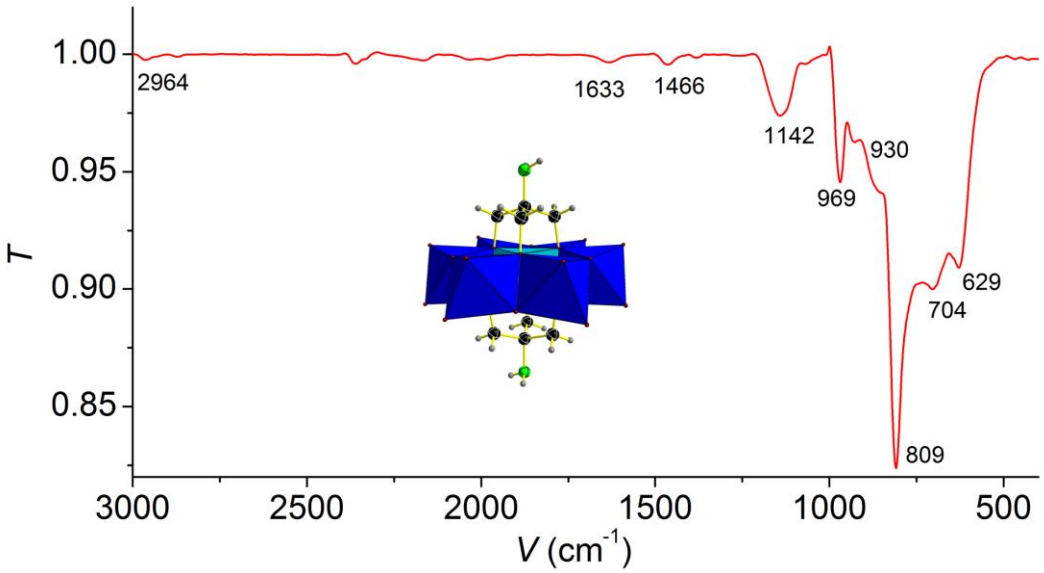

Figure S4. The FT-IR spectrum of $(NH_4)_4\{[NH_2C(CH_2O)_3]_2CuMo_6O_{18}\}$ cluster.

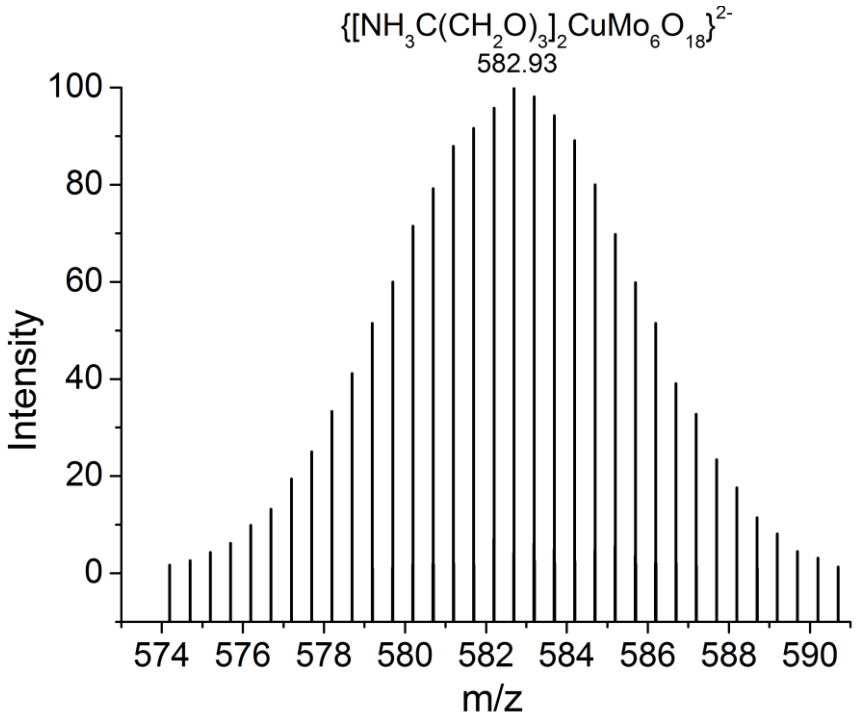

Figure S5. Negative-mode ESI-MS of $(NH_4)_4\{[NH_2C(CH_2O)_3]_2CuMo_6O_{18}\}$ cluster. The peak belongs to the protonated $\{[H_3NC(CH_2O)_3]_2CuMo_6O_{18}\}^{2-}$.

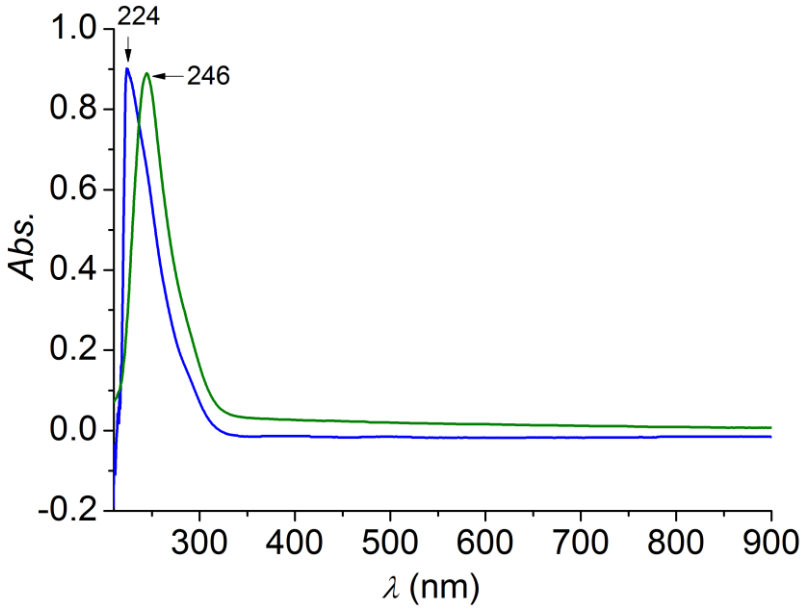

Figure S6. UV/Vis LMCT spectra of $(NH_4)_4\{[NH_2C(CH_2O)_3]_2CuMo_6O_{18}\}$ (246 nm) and $(NH_4)_4[Cu(OH)_6Mo_6O_{18}]$ cluster (224 nm).

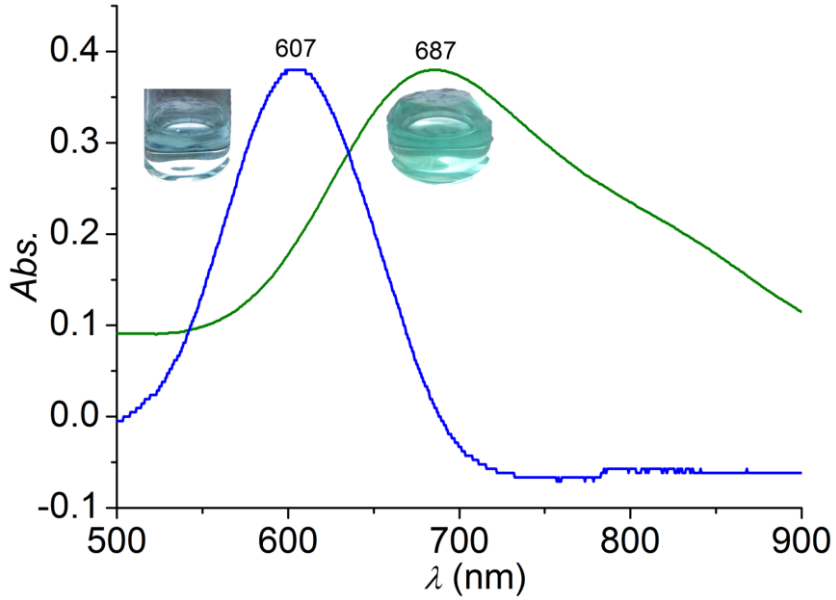

Figure S7. UV/Vis d-d transition spectra of $(NH_4)_4\{[NH_2C(CH_2O)_3]_2CuMo_6O_{18}\}$ (687 nm) and $(NH_4)_4[Cu(OH)_6Mo_6O_{18}]$ cluster (607 nm).

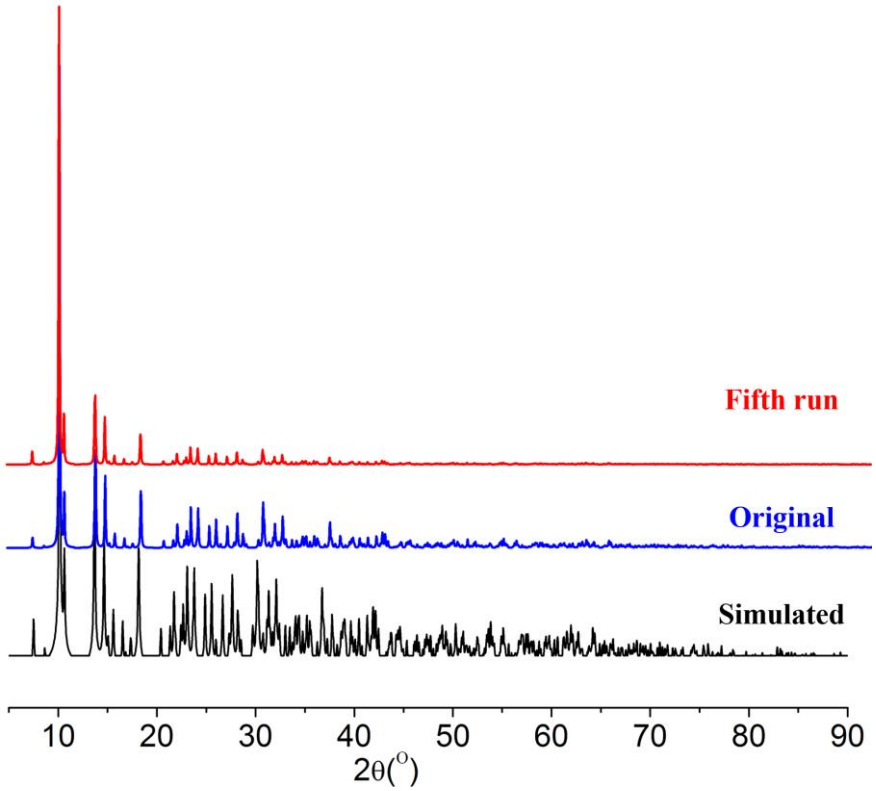

Figure S8. The simulated XRD of $(NH_4)_4\{[NH_2C(CH_2O)_3]_2CuMo_6O_{18}\}$, and powder XRD pattern of the as-obtained cluster and the cluster after fifth catalytic run. Simulation is based on the single crystal X-ray diffraction data.

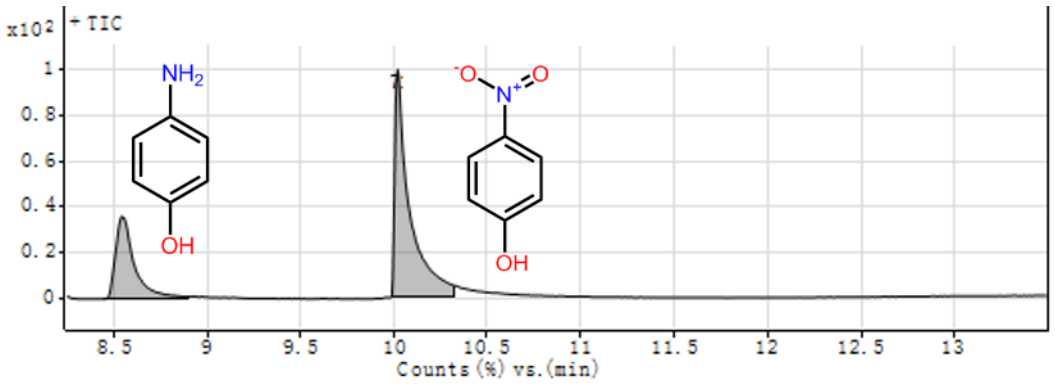

Figure S9a. Reaction process of *p*-nitrophenol reduction towards *p*-aminophenol generation monitored by GC-MS spectra at 3.5min

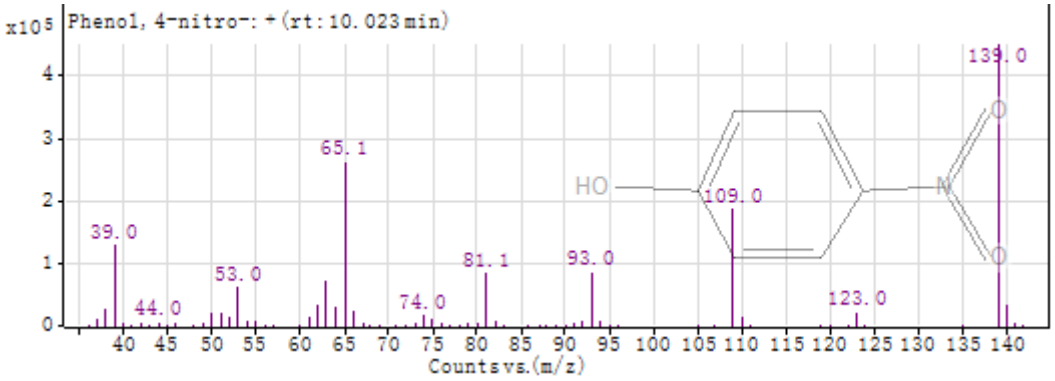

Figure S9b. Substance match of the reactant from the NIST mass spectral library through MassHunter

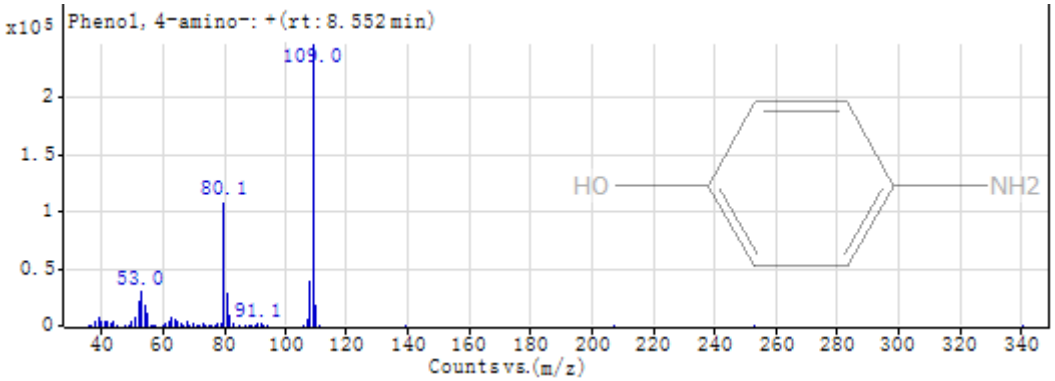

Figure S9c. Substance match of the product from the NIST mass spectral library through MassHunter

peaks	begin time(min)	retention time(min)	end time(min)	intensity	integral area	area percentage (%)
1	8.447	8.552	8.895	633174.94	4522184.91	31.6
2	9.982	10.018	10.318	1755162.93	9781712.67	68.4

Table S2. The peaks, retention time and integral area of the reactants p-nitrophenol and the corresponding product p-aminophenol from GC-MS spectra at 3.5min

Equation	$lnC_t=lnC_o-kt$		
Weight	No Weighting		
Residual Sum of Squares	1.53E-04	2.21E-04	1.37E-04
Pearson's r	-0.99996	-0.99996	-0.9999
Adj. R-Square	0.99987	0.99987	0.9997
		Value	Standard Error
$\{[NH_2C(CH_2O)_3]_2CuMo_6O_{18}\}^{4-}$	Intercept	0.214	0.01072
	Slope	-0.19513	0.0013
$[Cu(OH)_6Mo_6O_{18}]^{4-}$	Intercept	0.2568	0.01286
	Slope	-0.23416	0.00157
$[Mo_7O_{24}]^{6-}$	Intercept	0.13317	0.00901
	Slope	-0.02068	2.05E-04

Table S3. The linear fitting parameters of catalytic reaction kinetics equation

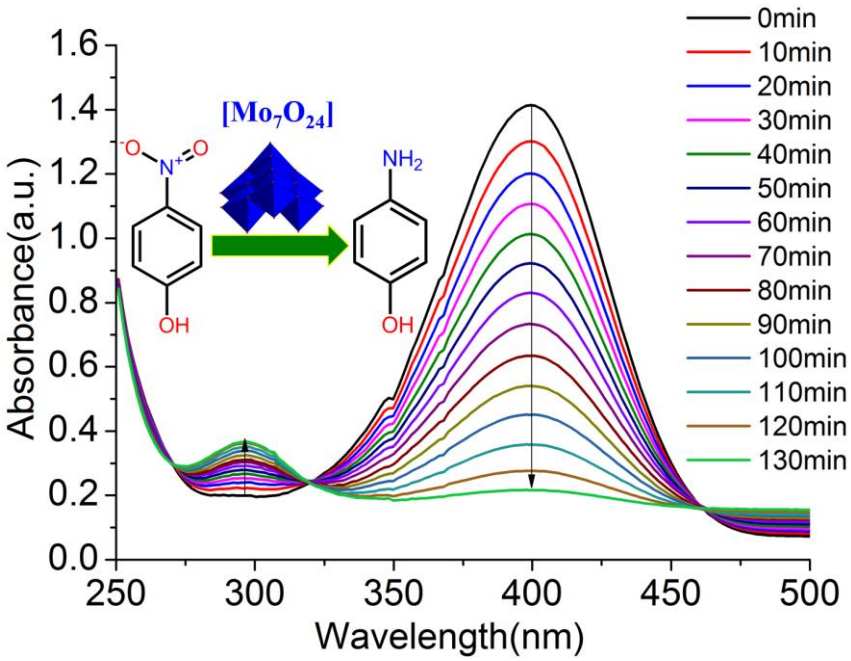

Figure S10. Reaction process of *p*-nitrophenol reduction towards *p*-aminophenol over the monometallic $(NH_4)_6[Mo_7O_{24}]$ catalysts.

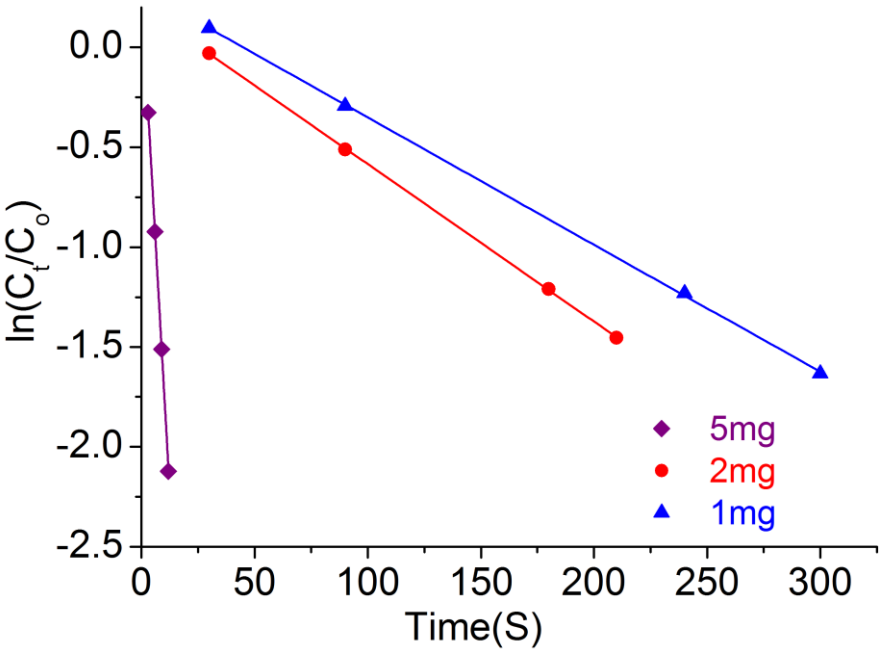

Figure S11. Catalytic reaction kinetics comparison of bimetallic $(NH_4)_4\{[NH_2C(CH_2O)_3]_2CuMo_6O_{18}\}$ catalyst with different amount.

Equation	$lnC_t=lnC_o-kt$		
Weight	No Weighting		
Residual Sum of Squares	8.62E-05	6.38E-05	2.49E-04
Pearson's r	-0.99998	-0.99997	-0.99994
Adj. R-Square	0.99993	0.99992	0.99981
		Value	Standard Error
5mg	Intercept	0.2742	0.00804
	Slope	-0.19928	9.79E-04
2mg	Intercept	0.20401	0.00577
	Slope	-0.00788	3.95E-05
1mg	Intercept	0.28633	0.01011
	Slope	-0.00637	5.11E-05

Table S4. The linear fitting parameters of catalytic reaction kinetics equation with bimetallic $(NH_4)_4\{[NH_2C(CH_2O)_3]_2CuMo_6O_{18}\}$ catalyst amount optimization.

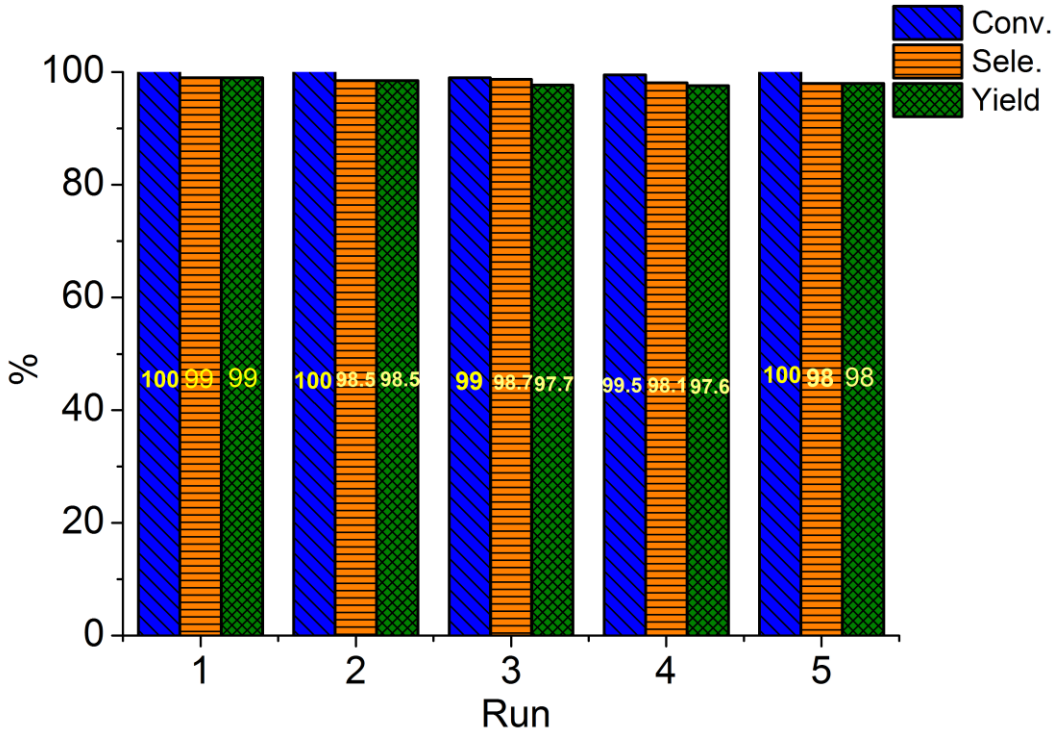

Figure S12. The conversion, selectivity and yield of *p*-nitrophenol hydrogenation reaction employ recovered $\{[NH_2C(CH_2O)_3]_2CuMo_6O_{18}\}^{4-}$ catalyst of five cycle runs

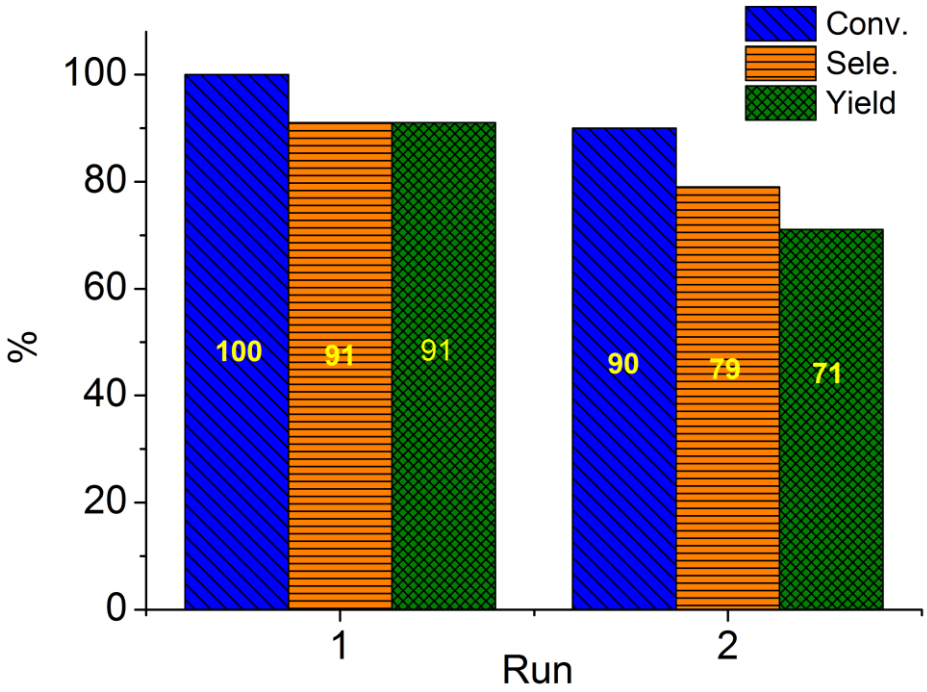

Figure S13. The conversion, selectivity and yield of *p*-nitrophenol hydrogenation reaction employ recovered $[Mo_7O_{24}]^{6-}$ catalyst of two cycle runs

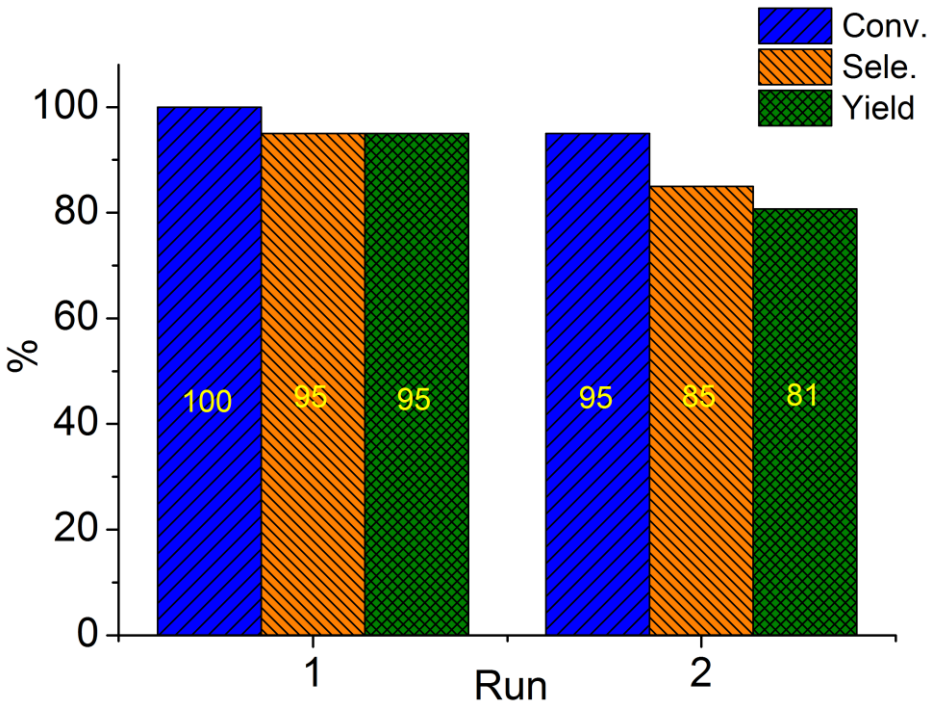

Figure S14. The conversion, selectivity and yield of *p*-nitrophenol hydrogenation reaction employ recovered $[Cu(OH)_6Mo_6O_{18}]^{4-}$ catalyst of two cycle runs

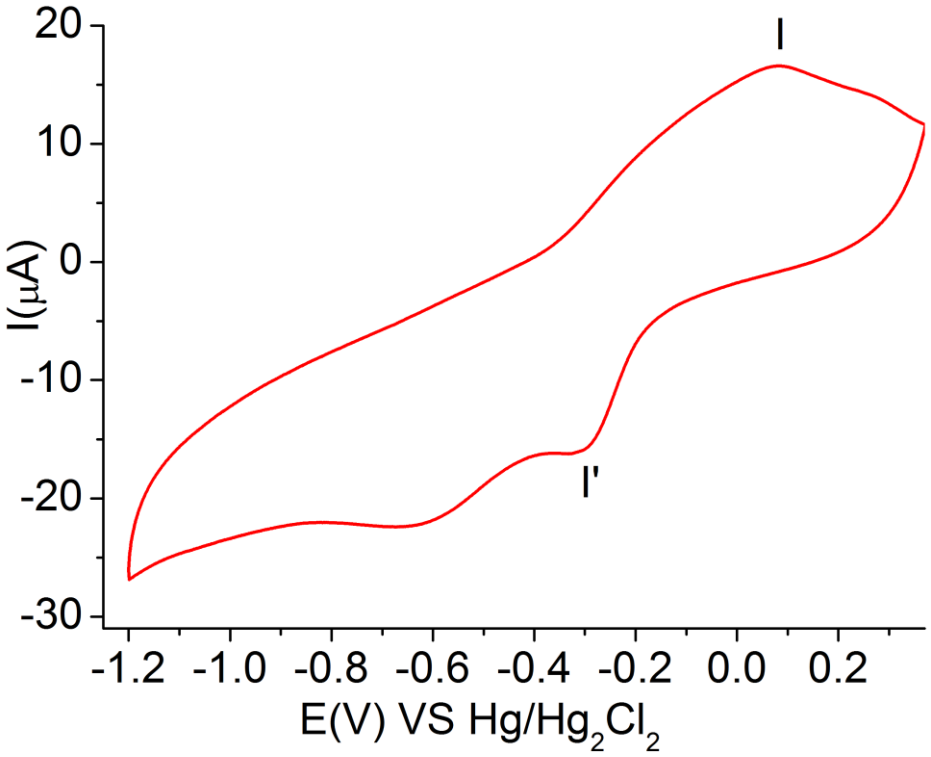

Figure S15 Cyclic voltammetry of tris ligand